Nanofibril Self-Assembly of an Arylene Ethynylene Macrocycle

Kaushik Balakrishnan,[†] Aniket Datar,[†] Wei Zhang,[‡,¶] Xiaomei Yang,[†] Tammene Naddo,[†]
Jialing Huang,[§] Jianmin Zuo,[¶] Max Yen,[§] Jeffrey S. Moore,*,[‡,¶] and Ling Zang*,[†]

*Department of Chemistry and Biochemistry, Southern Illinois University, Carbondale, Illinois 62901, Departments
of Chemistry and Materials Science and Engineering, 600 South Mathews Avenue, University of Illinois at
Urbana–Champaign, Urbana, Illinois 61801, and Materials Technology Center (MTC),
Southern Illinois University, Carbondale, Illinois 62901*

Received March 18, 2006; E-mail: lzang@chem.siu.edu; jsmoore@uiuc.edu

Nanostructured, one-dimensional (1D) morphologies composed of electronically active constituents are likely to become important in the fabrication of nanoscale optoelectronic devices. Due to their straightforward synthesis and unique molecular structure that includes large-area, shape-persistent π-surfaces, arylene ethynylene macrocycle (AEM) molecules have gained increasing interest, particularly for application in nanomaterials and nanodevices.[1–5] The large planar (or nearly planar) molecular surfaces of AEMs are expected to promote π–π stacking, thus enabling efficient intermolecular electronic coupling. We imagined that, under appropriate fabrication conditions, the strong π–π stacking inherent to AEMs would facilitate their spontaneous assembly into 1D nanofibrils. Indeed, strong π–π interactions have proven to be important for organizing AEMs in bulk states, including nanoporous crystals,[6–8] liquid crystals,[9–11] monolayers,[12] and single crystals.[13] To date, however, there have yet to be any reports on well-defined, 1D assemblies fabricated from AEM molecules. Here we report a robust, sol–gel method to fabricate nanofibril structures from an AEM molecule, **1** (Chart 1).

The main challenge in assembling large aromatic molecules into 1D materials lies in balancing the molecular assembly for growth along the π-stacking direction against the lateral association of side chains. The former dictates the 1D morphology of self-assembly, whereas the latter favors the formation of bulk assemblies. For AEMs, a simple fabrication method, such as molecular dispersion into a "poor" solvent or concentration via solvent evaporation, usually produces ill-defined agglomerates, rather than extended 1D structures. This favorable lateral growth is mainly driven by the strong, solvophobically favorable hydrophobic interactions between the long alkyl side chains.

Sol–gel processing is usually an effective way to decrease the molecular mobility (dynamics) and thus minimize the lateral growth of molecular assembly due to side-chain association. Slow cooling of a warm, homogeneous solution of **1** from high temperature to room temperature leads to gelation of the solution. Of all the solvents that were tested (e.g., chloroform, hexane, THF, methanol, cyclohexane, decline, etc.), only cyclohexane had the ability to induce gelation of **1**. As described below, the gelation process is accompanied by a high degree of supramolecular organization with optimal π–π stacking and in cooperation with the side-chain association.

Figure 1 shows the AFM images of the cyclohexane gel spin-cast on glass, followed by drying in air. Large-area scanning depicts the fibril piles composed of entangled nanofibrils and bundles, a morphological signature of that the gelating property of **1** is pri-
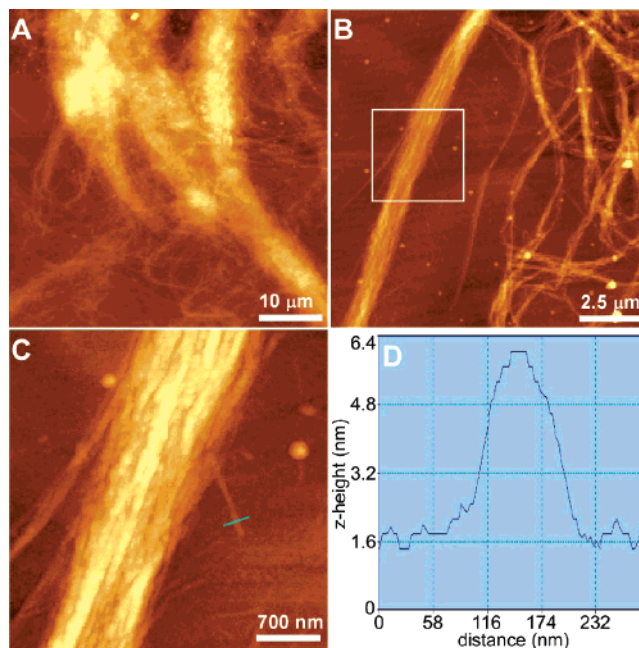
† Department of Chemistry and Biochemistry, Southern Illinois University.
‡ Department of Chemistry, University of Illinois at Urbana–Champaign.
§ Materials Technology Center, Southern Illinois University.
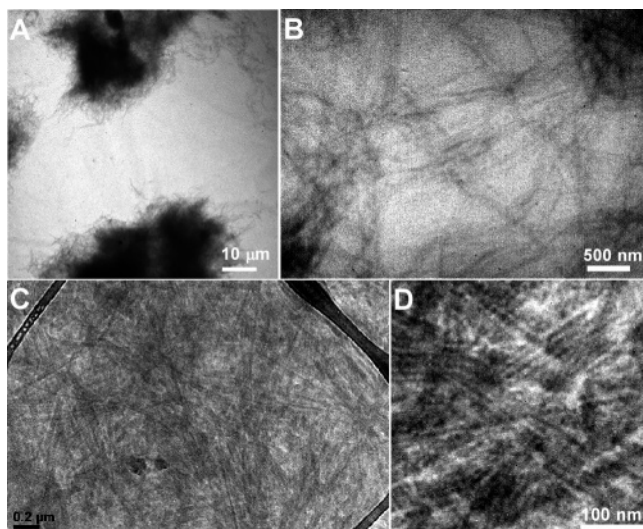¶ Department of Materials Science and Engineering, University of Illinois at Urbana–Champaign.

Figure 1. AFM images of the gel of **1** spin-cast and dried on glass: (A) large-area image showing the fibril piles; (B) different sizes of fibril bundles; (C) a zoomed-in image over a bundle marked in C; (D) z-height line scan profile over a single fiber marked in C. The total z-height ranges for A–C are 390, 49, and 28 nm, respectively.

Chart 1
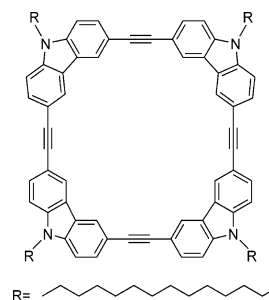
marily due to the columnar stacking of the macrocycles. The columnar stacking is also inferred from the X-ray diffraction of the gel (Figure S7), for which the diffractogram is dominated by a single sharp peak at low angle (characteristic of columnar stacked phase).[14] The d spacing corresponding to the π-stacking is calculated to be ca. 3.8 Å, which is consistent with the typical distance for effective π–π stacking between aromatic molecules. Due to the rigid, non-collapsible character of **1**, the nanofibril is likely to be a tubular, nanoporous arrangement of stacked rings. A zoomed-in image (Figure 1C) shows an individual fiber separated from a bundle. A

Figure 2. TEM images of the gel of AEM **1** deposited on silicon oxide (A, B) and holey carbon (C, D) films: (A) large-area image showing the fibril piles; (B) different sizes of fibril bundles; (C) highly uniform nanofibrils lying across a hole of the carbon film; (D) a zoomed-in image over the sample of C. The TEM samples were prepared by drop-casting of a diluted gel suspension in cyclohexane (~5% vol dilution).

Figure 3. Absorption (solid) and fluorescence (dotted) spectra of molecularly dissolved solution (black) and dried gel (red) of **1**. The solution was made in THF at 1 μM. Due to the scattering interference for absorption measurement of the gel sample, the fluorescence excitation spectrum (red solid) is plotted instead. All spectra are normalized to the max.

line scan over the single fiber indicates the cross section size to be ca. 4.5 nm, which roughly corresponds to the size of two molecules of **1** assembled laterally with full interdigitation of side chains (Figure S8). The lateral supramolecular assembly of other AEM has recently been observed on surfaces by STM.[4] Particularly for the AEMs with long alkyl side chains, the lateral supramolecular assembly is mainly due to the side-chain interdigitation.[15]

Diluting the gel into a medium-quality solvent, such as cyclohexane (which provides medium solubility for the molecule), produced well-dispersed fibrils as revealed by the TEM imaging (Figure 2). In contrast, when dispersed in a good solvent, such as chloroform or THF, the gel became completely redissolved, leading to a homogeneous solution. On the other hand, dispersion in a poor solvent, such as methanol, resulted in formation of large agglomerates due to the further aggregation of the molecular assemblies.

Consistent with the AFM measurement, a large-area TEM image (Figure 2A) reveals that the dried gel consists of piles of entangled nanofibrils. The strong $\pi-\pi$ stacking gives the fibril structure sufficient mechanical integrity to be transferred onto different substrates. Compared to the polar substrate of silicon oxide as used in Figure 2A and B, a holey carbon film (nonpolar) was also employed as substrate for TEM imaging of the nanofibrils (Figure 2C and D). For the nanofibers lying across a hole, the TEM image shows better contrast due to the ease of focus and astigmatism correction. This robust, durable character of the nanofibril (which allows for easy handling and deposition onto solid substrate) will be critical for approaching practical applications of the nano-assembly.[16]

Considering the fact that the electronic property of AEMs is principally determined by the conjugate structure of the cycle, it is interesting to observe the degree to which the $\pi-\pi$ interaction between the cycles perturbs electronic features. Such perturbation is closely correlated with the molecular stacking conformation, which in turn dictates the morphology of the molecular aggregates. Figure 3 shows the UV−vis absorption and fluorescence spectra of both the homogeneous solution and nanofibril aggregate of **1**. Upon aggregation, the strong $\pi-\pi$ interaction (i.e., electronic coupling) leads to quenching of emission of individual molecules and formation of new emission bands at longer wavelength. Consistent with the emission spectral change, the absorption
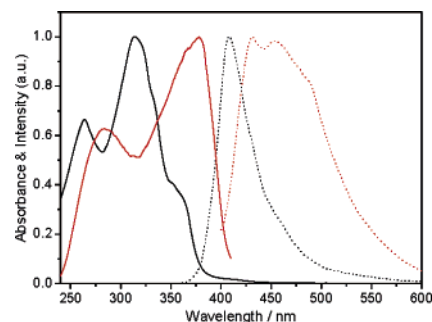
transition around 375 nm is relatively enhanced upon molecular stacking. These spectral changes are characteristic of a π-stacked molecular aggregate,[16,17] for which, like an excimer, the collective electronic features are significantly different from the individual component molecules.

In summary, nanofibril structures have been fabricated from an AEM molecule through a gelating process. The favorable 1D molecular assembly is likely due to the decreased mobility of molecules during the gelation, which minimizes the steric hindrance of side chains. The frame of **1** is highly rigid, π-conjugate, and in a totally planar conformation (Figure S8); the hydrogen-to-hydrogen distance across the frame interior is ca. 9.5 Å. One can therefore anticipate that 1D self-assemblies of **1** should produce a new type of nanomaterials with well-defined, noncollapsible internal channels,[9,18] which may provide interesting applications in nanoscale optoelectronic devices.

Supporting Information Available: Experimental details of nanofibril fabrication and microscopy characterization. This material is available free of charge via the Internet at http://pubs.acs.org.

References

(1) Moore, J. S. *Acc. Chem. Res.* **1997**, *30*, 402−413.
(2) Zhao, D.; Moore, J. S. *Chem. Commun.* **2003**, 807−818.
(3) Hoger, S. *J. Polym. Sci., Part A: Polym. Chem.* **1999**, *37*, 2685−2698.
(4) Grave, C.; Schluter, A. D. *Eur. J. Org. Chem.* **2002**, 3075−3098.
(5) Yamaguchi, Y.; Yoshida, Z.-i. *Chem.−Eur. J.* **2003**, *9*, 5430−5440.
(6) Venkataraman, D.; Lee, S.; Zhang, J.; Moore, J. S. *Nature* **1994**, *371*, 591.
(7) Hoeger, S.; Morrison, D. L.; Enkelmann, V. *J. Am. Chem. Soc.* **2002**, *124*, 6734−6736.
(8) Campbell, K.; Kuehl, C. J.; Ferguson, M. J.; Stang, P. J.; Tykwinski, R. R. *J. Am. Chem. Soc.* **2002**, *124*, 7266−7267.
(9) Mindyuk, O.; Stetzer, M. R.; Heiney, P. A.; Nelson, J. C.; Moore, J. S. *Adv. Mater.* **1998**, *10*, 1363−1366.
(10) Zhang, J.; Moore, J. S. *J. Am. Chem. Soc.* **1994**, *116*, 2655−2656.
(11) Hoger, S.; Enkelmann, V.; Bonrad, K.; Tschierske, C. *Angew. Chem., Int. Ed.* **2000**, *39*, 2268−2270.
(12) Shetty, A. S.; Fischer, P. R.; Stork, K. F.; Bohn, P. W.; Moore, J. S. *J. Am. Chem. Soc.* **1996**, *118*, 9409−9414.
(13) Ge, P.-H.; Fu, W.; Herrmann, W. A.; Herdtweck, E.; Campana, C.; Adams, R. D.; Bunz, U. H. F. *Angew. Chem., Int. Ed.* **2000**, *39*, 3607−3610.
(14) Bushey, M. L.; Hwang, A.; Stephens, P. W.; Nuckolls, C. *J. Am. Chem. Soc.* **2001**, *123*, 8157−8158.
(15) Pan, G.-B.; Cheng, X.-H.; Hoeger, S.; Freyland, W. *J. Am. Chem. Soc.* **2006**, *128*, 4218−4219.
(16) Hoeben, F. J. M.; Jonkheijm, P.; Meijer, E. W.; Schenning, A. P. H. J. *Chem. Rev.* **2005**, *105*, 1491−1546.
(17) Balakrishnan, K.; Datar, A.; Oitker, R.; Chen, H.; Zuo, J.; Zang, L. *J. Am. Chem. Soc.* **2005**, *127*, 10496−10497.
(18) Moore, J. S. *Nature* **1995**, *374*, 495−496.

JA0618550